BREADBOARD MODEL OF A CALORIMETRIC DEBRIS DETECTOR

M. Kobusch(1), F. Jäger(1), K.D. Bunte(2), T. Fichna(3)

(1) Physikalisch-Technische Bundesanstalt (PTB), Bundesallee 100, 38116 Braunschweig, Germany, michael.kobusch@ptb.de, frank.jaeger@ptb.de
(2) eta_max Space GmbH, Richard-Wagner-Str. 1, 38106 Braunschweig, Germany, k.bunte@etamax.de
(3) Institut für Datentechnik und Kommunikationsnetze (IDA), Technische Universität Braunschweig, Hans-Sommer-Str. 66, 38106 Braunschweig, Germany, t.fichna@tu-bs.de

ABSTRACT

This paper presents the breadboard model of a new type of in-situ space debris and meteoroid detector which determines the impact energy of micron-sized particles by calorimetric measurements. The detector utilises an array of small calorimeters. Each array element consists of an energy absorber and thermopile sensor which measures the temperature rise occurring after an impact.

1. INTRODUCTION

1.1. Objectives and Sensor Concept

A profound knowledge of Earth's particulate environment is essential for the establishment of reliable debris and meteoroid models which are applied for risk analysis and the development of effective shielding designs. In particular, the distribution and directional characteristics of small-sized particles is fairly unknown. Data about particle flux rate, size, mass, velocity or the related kinetic energy, respectively, is required as well as information about the particle's trajectory in order to determine the origin of the detected particle.

Small particles can only be investigated by in-situ detection or by means of the investigation of retrieved hardware. The latter is limited to certain orbital altitudes and yields the flux integrated over the exposure duration. Since existing in-situ detectors are not able to provide the required data and accuracy, the development of a new type of impact detector - AIDA - has been initiated [1]. Its design concept is based on a two-stage detector approach (c.f. Fig. 1), in which the velocity vector of an impacting particle is measured by the first stage and the impact energy by the second stage.

The development of the energy stage was carried out within the scope of an assessment study released by ESA/ESTEC in order to review and improve in-situ measurement techniques. This paper presents the developed calorimetric impact detector which uses an array of sensitive calorimeters for the measurement of impact energy as well as impact location. Due to the response time of a calorimetric detector, the detector cannot provide a high-resolution impact timing which would be needed for a velocity measurement stage. For this reason, the ARIEL impact ionisation detector by UniSpace Kent and The Open University, UK may be attached as an add-on detector stage in order to provide this timing data.

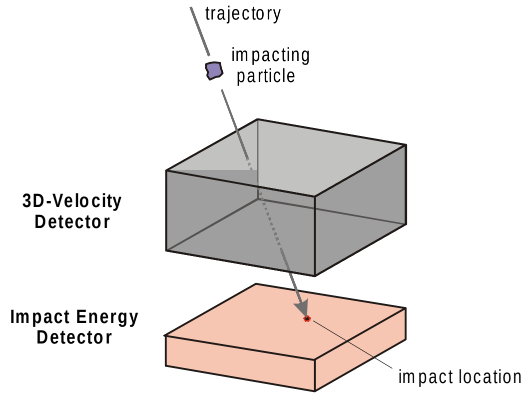

Figure 1. Schematic of the AIDA two-stage detector.

1.2. Principle of Calorimetric Impact-Heating

The calorimetric measurement is based on the fact that a substantial part of the kinetic energy E_{kin} of an impacting particle is converted into heat when hitting the target. Each calorimeter consists of an energy absorber and a temperature sensor measuring the impact-related temperature increase. For a maximum temperature rise and thus optimal sensitivity of the calorimetric sensor, the heat capacitance of the energy absorber should be as small as possible. Consequently, the presented breadboard model uses an array of small calorimeters (c.f. Fig. 2).

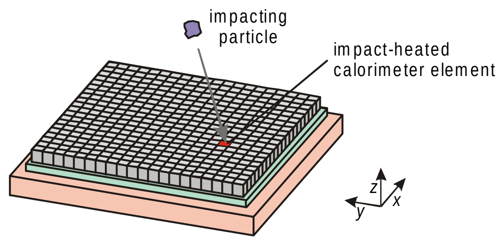

Figure 2. Array of calorimetric energy detectors.

Assuming an adiabatic heating of a calorimetric energy absorber of mass m_{A} and specific heat c_{A}, the deposed energy of the impacting particle results in a temperature increase of

Proceedings of the Fourth European Conference on Space Debris, Darmstadt, Germany, 18-20 April 2005
(ESA SP-587, August 2005)

$$\Delta T = \eta_{\mathrm{conv}} \cdot E_{\mathrm{kin}} \cdot \frac{1}{m_{\mathrm{A}} \cdot c_{\mathrm{A}}} \qquad (1)$$

Here, the factor η_{conv} describes the conversion efficiency between the kinetic energy E_{kin} of the impacting particle and the thermal energy deposed in the target matter. In reality, ejecta, impact plasma and radiation lead to some losses which don't contribute to the heating of the calorimetric mass. Because of sparse information about the conversion efficiency, realistic values have to be determined in experimental tests.

The following example gives a value for the expected temperature increase at the proposed detection threshold considering a particle of 10^{-14} kg (diameter about 2 µm) arriving at 10 km/s, thus having a kinetic energy of 500 nJ. Under the assumption of full energy conversion ($\eta_{\mathrm{conv}} = 1$), an absorber of 0.5 mg mass made of copper will be heated by 2.6 mK.

2. DESIGN AND MANUFACTURING OF THE BREADBOARD MODEL

2.1. Selection of the Temperature Sensor

The small temperature increase of the impact-heated absorber has to be measured by a sensitive sensor without introducing too much additional heat capacitance which would otherwise compromise the measurement performance. This requirement is met by miniaturised multijunction thermopile sensors usually used for the detection of infrared radiation at non-contact temperature measurements. These sensors offer high sensitivity, linearity, small size and fast response as well as insensitivity to changes of ambient temperature due to their measuring principle. Furthermore, their manufacturing process is based on silicon wafer technologies which allow the design of large sensor arrays on the wafer level scale.

A miniaturised thermopile sensor consists of a thin membrane of low thermal conductivity that spans over a thick silicon frame (Fig. 3). Both parts of the sensor are at different temperatures if the membrane is exposed to thermal radiation or contacted to a heat source. For the calorimetric detector presented in this paper, the thermal energy of an impact event heats the absorber which is thermally connected to the membrane's centre. The resulting temperature difference is transformed into a proportional voltage signal by a serial circuit of thermocouples, which have their hot and cold junctions situated on the membrane or on the silicon frame, respectively.

Resolution and detection threshold of the thermopile sensor is limited by the thermal noise voltage of its electrical resistance R. This noise voltage is

$$U_{\mathrm{Noise}} = \sqrt{4 \cdot \mathrm{k} \cdot R \cdot T \cdot \Delta f} \qquad (2)$$

where k is Boltzmann's constant (1.38 10^{-23} J/K), T is temperature and Δf is noise bandwidth. Noise can only be reduced by smaller bandwidths if an active cooling of the sensor is not applicable.

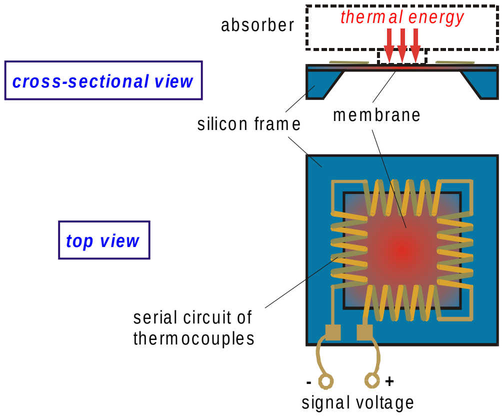

Figure 3. Principle of a thermopile sensor.

2.2. Design of the Thermopile Array

An array of 16x16 thermopile sensors was chosen for the breadboard model. These 256 sensors cover a total detection area of about 33 square centimetres. The array design is based on the thermopile sensor TS-100F of IPHT Jena (Institute for Physical High Technology). In order to keep the element size small, the sensor spacing of the original single chip layout was not changed. A TS-100F sensor chip measures 3.6 mm x 3.6 mm and has a membrane area of 2.2 mm x 2.2 mm (c.f. Fig. 4). Its radially arranged circuit of 100 thermocouples connected in series generates a total thermopower of about 13 mV/K. The sensor features an integrated electric heater designed as a circular meander-shaped circuit path at the membrane's centre. Applying a heater signal under vacuum conditions, a time constant of 220 ms was measured for the thermopile. This heater is intended for calibrations purposes and would give the opportunity of health monitoring in space.

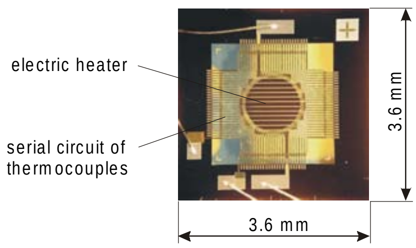

Figure 4. TS-100F thermopile sensor by IPHT.

The new design required a complete modification of the existing layout mask set for 4" wafers including new circuit paths and contact pads. The top surface now features small spacers (height of 20 µm) made of insulating polymer in order to keep a minimum distance between absorber and membrane. Thus, in case of some warping of a thin absorber, an undesired thermal bypass due to additional contact spots is avoided.

The electrical layout design of the 16x16 thermopile array is depicted in Fig. 5. It consists of multiple 1x8 linear sensor arrays. A total of 800 bond pads belonging to 256 individual thermopile sensors and 256 heaters are arranged at two sides of the array chip. The 8 heaters of each sensor line are connected to common ground.

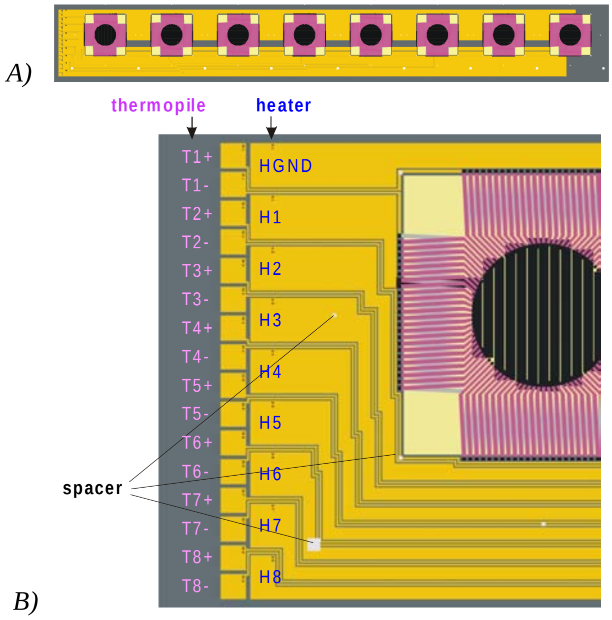

Figure 5. Layout of the 16x16 thermopile array: 1x8 linear sensor array (A), bond pads and spacers (B).

2.3. Design of the Absorber Array

A matching absorber array of 256 elements, which are thermally isolated against each other, has to be applied to the thermopile array by thermal glue. Considering a fill-factor of almost unity, each absorber element has a detection area of 3.6 mm squared. For a given material and structural density, the heat capacitance of the absorber is mainly a function of its thickness. The additive contribution resulting from the thermal glue has to be taken into account for very thin structures.

To achieve a calorimetric signal response independent of impact location, a plane plate absorber design was chosen. Metals like silver (Ag), gold (Au) and copper (Cu) are well suited materials because of their high thermal conductivity and relatively small specific heat. A thin top layer of low density polymer might be applied in order to reduce impact losses. Thin metallic plate absorbers of about 5 µm thickness are sufficiently thick to withstand an impact of a micron-sized particle and would also achieve the required sensitivity. Generally, the sensitivity range of the sensor can be adjusted by the absorber plate thickness.

The geometry of the designed metallic plate absorber array is visualised in Fig. 6. For a gap of 50 µm, the plates measure 3.55 mm x 3.55 mm. They are connected at their edges by small connectors in order to improve handling and mounting. The edge connectors lead to a small thermal bypass resulting in a cross-talk between adjacent sensor elements. For very big impacts actually destroying the hit element, a cross-talk analysis might reveal useful information about the impact energy.

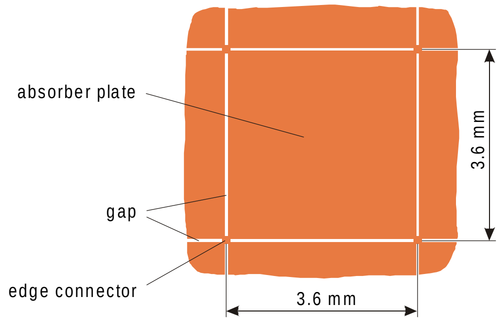

Figure 6. Design of the plate absorber array.

The thermal energy flow of the calorimeter array including thermopiles, glue and plate absorbers has been simulated by finite element methods (ANSYS). An example of a simulated non-central impact on the central element of a 3x3 array is given in Fig. 7. The images visualise a heat deposition of 500 nJ on a Cu-plate of 5 microns thickness 50 ms after impact. The hit plate nearly reaches an almost uniform temperature distribution after that time. At the edge connectors, some heat flows to the adjacent absorbers. The top view (A) shows the absorber plates, the bottom view (B) the sensor membranes. In addition to the visualisation of the heat distribution, temperature values can be extracted at the node positions of the structural finite element mesh.

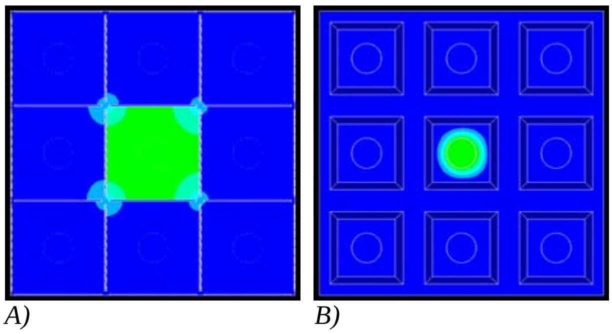

Figure 7. Thermal FE simulation of a 3x3 thermopile array with glued Cu-absorbers of 5 µm thickness: top view (A), bottom view (B), non-central heat deposition of 500 nJ on absorber plate after 50 ms.

2.4. Manufacturing of the Absorber Array

Two different manufacturing techniques for metallic plate absorber arrays have been successfully tested at PTB, namely lithography-based electroplating and laser cutting.

The first method utilises clean room techniques for the precise manufacturing of the desired structure. First, the outlines of the plate array are created by electron beam lithography (EBL) on an oxidised silicon wafer substrate. Then, the initial metallic seed layers are reinforced by electroplating.

Before structuring the front-side, the wafer's back-side was structured with a chromium mask in order to perform a back-side etching of the silicon resulting in a separated plate array that is still fixed at the remaining wafer frame. This frame can be handled for further processes like spin-coating of polymer layers, for example. The different process steps for the lithography-based electroplating of metallic plate absorber array are: spin-coating of photoresist (1), electron beam exposure (2), developing of photoresist (3), vacuum deposition of chromium (4) and gold (5) and a final lift-off process (6). Now, the front-side bears a thin metallic seed layer that can be electroplated to the desired thickness (7). Array and substrate are then separated by etching of the oxidised silicon wafer: HF etching of SiO_2 at the back-side (8), KOH etching of the silicon bulk (9), HF etching of SiO_2 at the front-side (10).

Electroplating of gold was performed with a galvanic bath yielding a purity of 99.9 % Au. Earlier experiments demonstrated that high purity is needed in order to avoid internal stress. The mean thickness of the gold layer was determined from the wafer's weight increase due to the galvanic process. The microphotography of Fig. 8A visualises the accurate structural definition of the manufacturing process. It shows the edge connector of four adjacent Au-plates of 5 µm thickness and separated by 50 µm wide gaps.

The second manufacturing method investigated is laser cutting. The desired plate array structure was cut into a thin metal layer using a pulsed UV laser system of 355 nm wavelength, a frequency tripled Nd:YVO4 laser (Neodymium Doped Yttrium Vanadium Oxide). This metal layer (e.g. Cu, Ag, Au) of specified thickness was sputtered onto a flat aluminium substrate of mirror surface quality in order to obtain a stress-free structure. The final separation of absorber array and substrate was achieved by etching. A microphotography of the obtained array structure is shown in Fig. 8B. Smaller magnifications show that the front surface is slightly darkened near the ablated gaps, thus the array structure is more obvious to the naked eye (c.f. Fig 12).

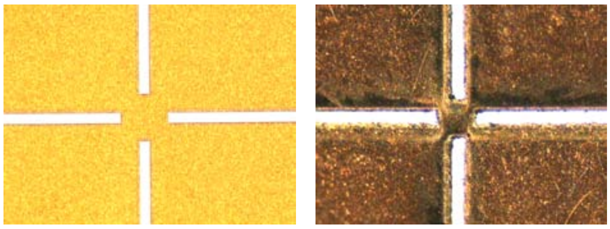

A) B)

Figure 8. Microphotographs of edge connectors of thin plate absorbers: A) Au-absorbers (5 µm thickness) made by lithography-based electroplating, B) Cu-absorbers (7 µm thickness) made by laser cutting.

2.5. Electronics Board

The data acquisition board of the breadboard model has to monitor 256 calorimeter elements simultaneously. By simplifying the basic signal circuit through an appropriate wire bonding of the thermopile wafer, the quantity of required electronic components could be substantially reduced. An inverse-series arrangement of each two thermopile sensors halves the number of channels to 128 and a parallel operation of each four heaters further reduces the number of circuit paths.

In order to make modifications of the electronics and the sensors more feasible, the thermopile array wafer with its absorbers is mounted onto an interchangeable sensor adapter board. Two zero insertion force (ZIF) sockets connect this adapter board to the electronics main board. This multilayer PCB is assembled with analog amplifiers, filters and multiplexers on both sides, as well as a microcontroller with build-in analog-to-digital converter (ADC) and an USB port controller to communicate with the controlling PC. The overall block diagram of the electronics board is depicted in Fig. 9.

Each channel features a band pass amplifier consisting of a 6 dB high pass followed by a 12 dB low pass (c.f. Fig 10). Their corner frequencies of 1 Hz and 30 Hz, respectively, are adapted to the thermopile's transient response and the expected influence of signal drifts due to thermal changes. The low pass suppresses signal noise and maintains the Nyquist criterion, whereas the high pass eliminates signal drift. Because of the high impedance of the thermopile couple of about 60 kΩ, the input filter first performs an impedance conversion with a gain of 15 before the second filter with a gain of 10 gives the required gain of 150. Multiplexers lead the filtered signals to a 16 bit AD-converter of 2.4 V input voltage which is integrated part of the microcontroller C8051F064 from Silicon Laboratories. Due to the virtual ground and the gain of 150, the corresponding thermopile signal voltage range is ±8 mV, the resolution is 0.244 µV or – with a sensor sensitivity of 13 mV/K – 18.8 µK, respectively. The microcontroller performs a quasi in parallel sampling of all 128 channels at the

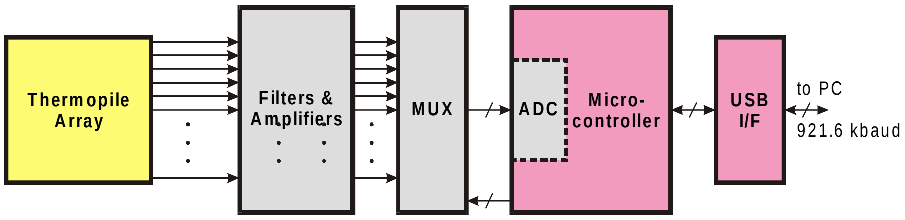

Figure 9. Overall block diagram of the measurement electronics.

envisaged rate of 75 samples/s and sends all raw acquisition data via USB port to the controlling PC.

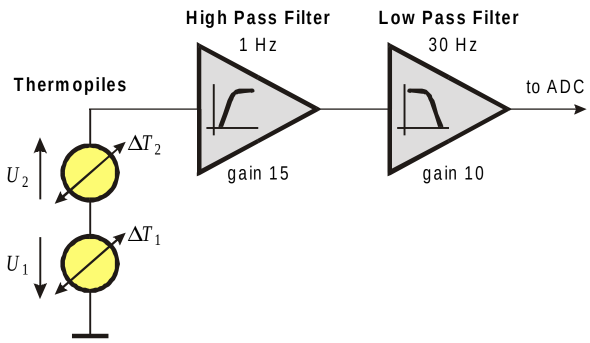

Figure 10. Block diagram of filter and amplifier chain.

The measurement range of the calorimetric detector is estimated for a 5 µm thick absorber plate made of copper, i.e. 0.56 mg mass and heat capacitance of 0.22 mJ/K. The detection threshold is defined by the thermal noise of the thermopile couple (R = 60 kΩ) according to Eq. 2. For a bandwidth of 29 Hz, a temperature of 323 K and a minimum signal-to-noise ratio of 3, the smallest detectable thermopile signal is about 0.53 µV or 2.2 digits. This voltage corresponds to a calorimetric input heat of 10 nJ or - in terms of impactor properties - to a particle of $4\cdot10^{-16}$ kg mass (0.5 µm iron sphere) at 10 km/s assuming a conversion efficiency of 50 %. On the other hand, the largest thermopile signal without clipping (8 mV or 32768 digits) corresponds to an input heat of 0.15 mJ.

2.6. Data Acquisition Software

Board control and functional tests of the breadboard model are performed by a special data acquisition and analysis software that has been developed with the GSEOS V 5.0 (Ground Support Equipment Operating System) software package of IDA. GSEOS was designed in order to support all stages of experiment development, from bench checking and spacecraft integration up to “quick-look” during flight operation. The latest GSEOS version runs under the operating systems Windows NT/2000/XP on INTEL PC platforms which are cost effective, widespread and support multiprocessing.

All 128 channels are monitored simultaneously at 75 samples per second. Selected channels can be graphically displayed online and saved on hard disk. The visualised noise distribution permits the evaluation of signal quality. Heater pulses of different energies can be applied to selected heater groups. A screenshot of this software is shown in Fig. 11.

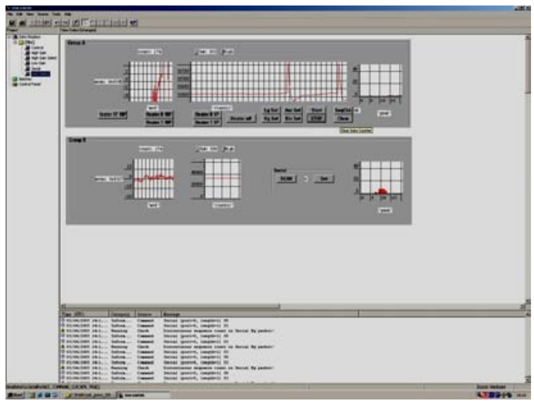

Figure 11. Screenshot of the data acquisition software.

2.7. Breadboard Model Integration

The mechanical assembly of the sensor array consists of four basic steps. First, the thermopile array wafer has to be glued onto the sensor adapter board. This process has to assure a ventilation of the wafer backside in order to tolerate vacuum conditions. The second step involves the connection of the absorber array consisting of 256 edge-connected metallic plates and the thermopile array by thermal glue. Well-proportioned droplets of less than 0.01 cubic millimetre volume have to be placed at the centre of the thermopile membranes. Third, the thermopile array wafer has to be wire bonded to the sensor adapter board of the breadboard model. At last, the electrical connection of sensor adapter board, electronics board and PC completes the sensor assembly.

The processes of model integration have to be optimised and automated for the engineering of flight models. For example, future thermopiles arrays will experience an automated bonding of its 800 contact pads and ceramic boards of similar thermal expansion coefficient as silicon will be used in order to minimise thermal stress.

The fixing of a large absorber array requires an automated proportioning and placing of glue droplets. A secure handling and positioning of the absorber array might be provided by vacuum mounting fixtures. Due to volume and weight restrictions, the detachable adapter board using ZIF sockets has to be replaced for future models.

The photograph of Fig. 12 shows the operating breadboard model equipped with two absorber arrays of different type. The 16 element array at left consists of Au-plates of 5 µm thickness, whereas the 9 element array at centre uses 7 µm thick plates made of copper.

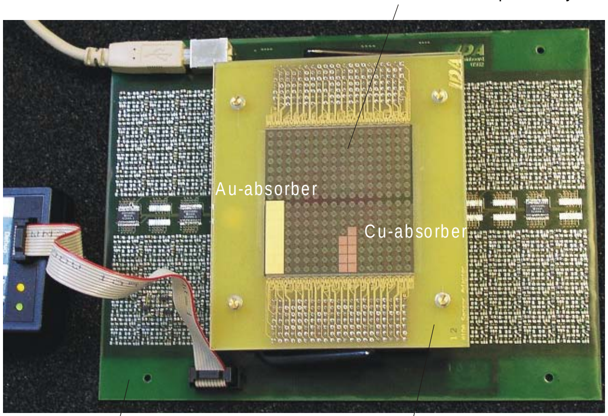

Figure 12. Assembled breadboard model with applied plane absorber arrays.

3. INITIAL FUNCTIONAL TESTS

First functional tests with thermal energy depositions in air have been successfully performed. The calorimeter element under test was heated by a laser light pulse of specified energy. This method offers high accuracy if laser pulse energies and absorption properties of the absorbers are well-known. Furthermore, it can be applied easily for the calibration of large detector arrays.

The tests utilised a pulsed diode laser of 0.5 mW optical output and 2 ms pulse widths. Incident pulse energies of 1 µJ were easily detected by a calorimetric Au-absorber of 5 µm thickness. A typical signal of such a laser pulse heating is shown in Fig. 13.

The characteristic signal shape is the result of the calorimeter's decaying step response in air filtered by the band pass configuration using 1 Hz and 30 Hz corner frequencies. At vacuum conditions, the longer decay time will lead to noticeably broader pulses. Assuming an absorption coefficient of less than 20 % for slightly oxidised copper surfaces, the deposed thermal energy was smaller than 200 nJ. This example clearly demonstrates the excellent heat detection capability of the calorimetric sensor.

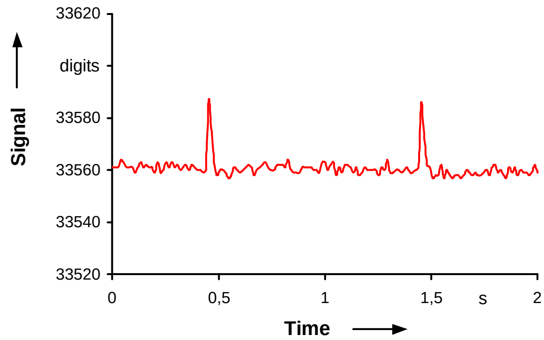

Figure 13. Measured calorimeter signal for laser pulse heating with pulses of 1 µJ optical output energy, absorbed energy < 200 nJ (estimation).

4. CONCLUSIONS AND OUTLOOK

After having successfully performed initial tests using laser pulse heating, hyper velocity impact (HVI) tests will prove the capabilities of the calorimetric energy detector in the next months. Here, valuable information about the widely unknown energy conversion efficiency is expected from experiments with different absorber materials. Further tests like vibration tests will validate the structural integrity of the developed detector. At the same time as the different processes for manufacturing, model integration and data analysis will be optimised with regard to a space qualified version of the AIDA impact detector, it is intended to look for flight opportunities as soon as possible.

ACKNOWLEDGEMENTS

The breadboard model was developed within the scope of the ESA/ESTEC Contract 17997/03/NL/JA. The thermopile array was designed and manufactured by IPHT Jena; the authors like to thank Dr. Keßler for his engagement. We also gratefully acknowledge the substantial contributions of our colleagues.

REFERENCES

[1] AIDA – An Advanced Impact Detector Assembly, K.D. Bunte, M. Kobusch, J. Hollandt, J. Illemann, F. Jäger, M. Gläser, S. Sarge, International Astronautic Congress 2003, Bremen, Germany.